



## Large-Scale First-Principles Calculations of Magnetic Nanoparticles

M. E. Gruner, G. Rollmann, P. Entel

published in

*NIC Symposium 2008*,  
G. Münster, D. Wolf, M. Kremer (Editors),  
John von Neumann Institute for Computing, Jülich,  
NIC Series, Vol. **39**, ISBN 978-3-9810843-5-1, pp. 161-168, 2008.

© 2008 by John von Neumann Institute for Computing  
Permission to make digital or hard copies of portions of this work for  
personal or classroom use is granted provided that the copies are not  
made or distributed for profit or commercial advantage and that copies  
bear this notice and the full citation on the first page. To copy otherwise  
requires prior specific permission by the publisher mentioned above.

<http://www.fz-juelich.de/nic-series/volume39>

# Large-Scale First-Principles Calculations of Magnetic Nanoparticles

Markus Ernst Gruner, Georg Rollmann, and Peter Entel

Fachbereich Physik, Universität Duisburg-Essen, 47048 Duisburg, Germany  
E-mail: {Markus.Gruner, Peter.Entel}@uni-due.de

Modern supercomputers as the IBM Blue Gene/L provide the possibility to investigate large systems containing several hundred transition metal atoms. We present results on two examples, the size dependent evolution of structure and magnetism of elemental iron nanoparticles and the identification of structural comparison of competing morphologies of near-stoichiometric Fe-Pt and Co-Pt nanoparticles, which are currently discussed as media for future ultra-high density recording applications.

## 1 Introduction

Transition metal nanoparticles are of growing interest, from the fundamental science point of view<sup>1,2</sup> as well as for technological applications.<sup>3,4</sup> Atomistic simulations of materials properties of nanometer sized objects can easily be carried out by classical molecular dynamics simulations using empirical model potentials which already permit simulations on mesoscopic length scales. In many cases, however, the relevant properties are related to the electronic structure, so that a quantum-mechanical approach is necessary. The recent evolution of supercomputing power allows for an *ab initio* treatment of systems in the nanometer size regime. This comes at hand for technological applications where the miniaturization of functional units plays an important role. Within this contribution, we present two examples in which large scale *ab initio* calculations contribute to resolve open questions in this field.

## 2 Computational Method

The density functional theory (DFT) provides a suitable way to calculate the properties of systems containing several hundreds or even a few thousands of atoms from first principles, i. e. from quantum-mechanical grounds. According to the theorem by Hohenberg and Kohn,<sup>5</sup> the ground state of the electronic system can be uniquely described as a functional of the electron density. The resulting equations are solved in a self-consistency approach. The exact form of the exchange-correlation part of the functional is not known; nevertheless, this approach has proven its validity with overwhelming success.<sup>6</sup> During the last decades, the DFT approach has been implemented and consecutively refined in a vast number of commercial and freely available codes. In our calculations, we use the Vienna *Ab initio* Simulation Package (VASP),<sup>7</sup> which has proven in many examples to provide an excellent compromise between speed and accuracy, using the projector augmented wave approach<sup>8</sup> to describe the interaction with the nuclei and the core electrons. The clusters were placed in a cubic supercell, surrounded by a sufficient amount of vacuum to prevent interactions with the periodic images;  $k$ -space integration was restricted to the  $\Gamma$ -point. For

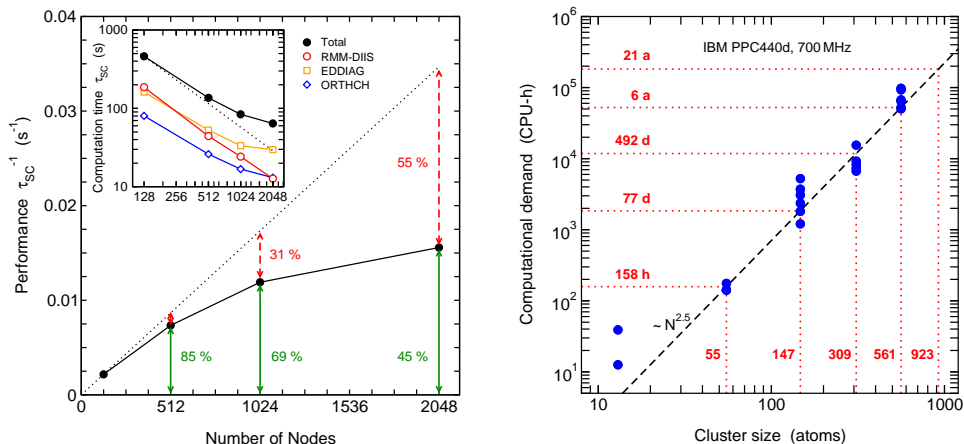


Figure 1. Left: Scaling behaviour of a nano-cluster with 561 Fe atoms on the IBM Blue Gene/L. The performance given by the inverse average computation time for an electronic self-consistency step,  $\tau_{SC}^{-1}$ , is shown as a function of the number of nodes (black circles). The dashed lines describe the ideal scaling behaviour. The inset shows a double logarithmic plot of  $\tau_{SC}$ . The open symbols in the inset refer to the scaling of the most time consuming subroutines. Right: Double logarithmic plot of the computation time per CPU needed on JUBL for a full geometric optimization of Fe-Pt nanoclusters of magic cluster sizes according to Eq. (1).

the exchange-correlation functional, we employed the generalized gradient approximation (for further details, refer to Refs. 9–12).

DFT calculations of large systems are not only time-consuming but also very demanding with respect to I/O bandwidth and memory. Thus the distribution over hundreds or thousands of CPUs is necessary to successfully complete such problems, especially on machines with hard limitations concerning CPU speed and memory per node as on the Blue Gene/L. Here, however, the threefold high-bandwidth, low-latency network helps to increase scalability so that large systems can be handled efficiently. Fig. 1 (right) shows as an example the scaling behaviour for an Fe<sub>561</sub> cluster (4488 valence electrons) where on 1024 nodes still 70 % of the ideal (linear scaling) performance is reached. The largest calculations carried out by our group contained 8000 valence electrons and ran with sufficient efficiency on four Blue Gene/L racks (4096 nodes). The DFT approach does not only yield total energies and electron densities, also forces can be calculated accurately. This allows for quasi-static structure optimizations which we perform on the Born-Oppenheimer surface, i. e. in the electronic ground state of the system. This requires to fully converge the electronic system before making an ionic movement. In VASP, an efficient prediction scheme for the new wavefunctions is implemented. Nevertheless, a considerable number of electronic self-consistency steps – for larger systems typically several thousands – have to be performed to find one meta-stable minimum on the potential energy surface. Figure 1 (right) shows the evolution of the required computation time for a complete geometric relaxation as a function of the size of the system. A pragmatic fit to a power law yields an increase of the computation time with system size with an exponent of about 2.5.

The systematic scan of the potential energy surface in order to find the most stable morphologies is a very demanding task even for small clusters containing a few tens of

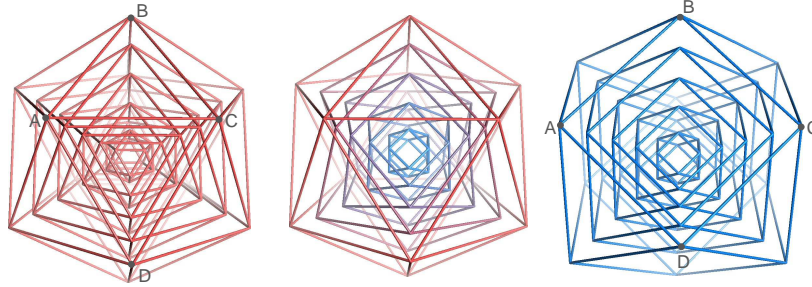


Figure 2. Edge models of the optimized  $\text{Fe}_{561}$  icosahedron (left), cuboctahedron (right) and SMT isomer (center). Separately for each shell, the corner atoms of the faces are connected by lines, the atoms themselves are omitted for clarity. For icosahedra and cuboctahedra, shells of the same shape but different sizes are stacked into each other. For the SMT isomer, the shape of the outermost shell is icosahedral and changes towards the inside continuously along the Mackay-path to a cuboctahedron, which represents the shape of the innermost shell. The Mackay transformation works by stretching the bond  $\overline{AC}$  of the icosahedron and turning the two adjacent triangular faces  $ABC$  and  $ACD$  into the same plane producing the square face  $ABCD$  of the cuboctahedron.

atoms. However, it becomes hopeless in the nanometer range. Therefore, a permissible way out is to restrict to an “educated guess” of selected morphologies. So-called magic-number clusters are a good starting point. Their size  $N$  is given as a function of the number  $n$  of closed geometric shells:

$$N = 1/3 (10n^3 + 15n^2 + 11n + 3) = 13, 55, 147, 309, 561, 923, \dots \quad (1)$$

Magic cluster sizes appear to be particularly stable for the late  $3d$  elements.<sup>13</sup> In addition, they allow for a comparison of several paradigmatic geometries: Cuboctahedra with a face centred cubic (fcc) structure, body centred cubic (bcc) isomers (Bain-transformed cuboctahedra), Mackay-icosahedra<sup>14</sup> and Ino-decahedra<sup>15</sup>.

### 3 Structure and Magnetism of Elemental Iron Nano-Clusters

As a bulk material, iron belongs certainly to the most important elements in everyday life. Many application are related to its magnetic properties. Iron possesses a complex structural phase diagram, with bcc  $\alpha$ - and  $\delta$ -phases below 1185 K and above 1167 K, the fcc  $\gamma$ -phase in between and the hexagonal close packed (hcp)  $\epsilon$ -phase at high pressures. Also, iron nanoparticles provide an interesting research field, too, due to their applicability in biomedicine (see, e. g., Ref. 16), but also from a fundamental point of view, since the evolution of their structure as a function of particle size has not been resolved so far: Transmission electron micrographs (TEM) of 6 nm particles suggest a bcc structure,<sup>17</sup> while for 13 atoms, first principles calculations predict a Jahn-Teller distorted icosahedron.<sup>18</sup> Recently the authors addressed this problems within a large scale *ab initio* approach which revealed that already above a crossover size of about 150 atoms the bulk-like bcc structure is energetically favored.<sup>11</sup> Furthermore, another important previously unreported structural motif was identified. The so-called shellwise Mackay transformed (SMT) isomer evolves by geometric relaxations from ideal icosahedra and cuboctahedra, if small distortions along the Mackay path<sup>14</sup> are imposed (cf. Fig. 2). Thus, for the case of iron, both geometric forms

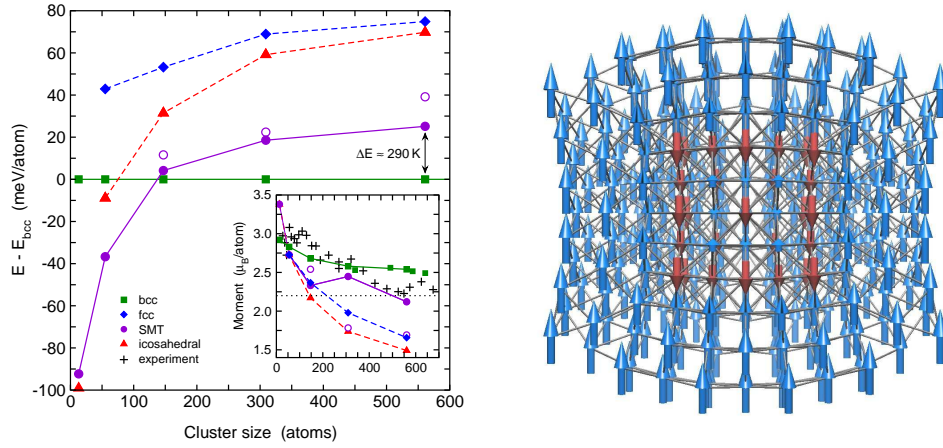


Figure 3. Left: Comparison of the energies of various isomers of elemental iron nano-clusters as a function of their size (data originally published in Ref. 11). The bcc isomer has been chosen as reference. Open symbols denote SMT isomers with magnetic configurations higher in energy. The lines are intended as guide to the eye, broken lines refer to unstable structures. The inset shows the variation of the average magnetic moment of the different isomers with size (experimental moments taken from Ref. 1). Right: Spin configuration of the lowest energy  $\text{Fe}_{561}$  SMT isomer (cross section). The arrows refer in length and orientation to the atomic moments.

must be considered unstable even for small cluster sizes. The comparison of the total energies of the different morphologies in Fig. 3 shows that the SMT isomer is a hot candidate for the ground state of  $\text{Fe}_{55}$ . Even up to 561 atoms, the energy difference between the bcc and the SMT isomer remains – in contrast to the cuboctahedra and icosahedra – in the range of thermal energies; thus the occurrence of the SMT structure appears realistic at finite temperatures. The calculated magnetic moments can be directly compared with the measurements on small transition metal nanoparticles by Billas *et al.*<sup>1</sup> (inset of Fig. 3). In accordance with a previous DFT study on clusters of up to  $N = 400$  atoms,<sup>2</sup> the moments of the bcc clusters agree very well with experiment in this size range. For larger clusters, however, considerable deviations occur. In fact, for  $N = 561$ , the SMT isomer shows the best agreement with the experimental magnetization data, owing to a shell-wise antiferromagnetic configuration of the cluster core.

The search for the origin of this unusual transformation requires an inspection at the atomistic level, which may become a tedious or even impossible task for large system sizes. In our case, help comes from the common neighbour analysis (CNA),<sup>19</sup> which has become a widely used tool for the identification of structural patterns in classical molecular dynamics studies of large systems. The CNA characterizes the local environment of an atom by a set of signatures, which can be compared with the characteristic result for an ideal bulk or surface structure. If one restricts to the first neighbour shell, signatures are obtained for each pair of neighbours, containing information on the number of nearest neighbours both atoms have in common, the number of bonds between these neighbours and the longest chain connecting them. Figure 4 shows the result of a CNA applied on optimized isomers. While the bcc and fcc clusters are uniform in structure, we find for the icosahedron the typical mixture of fcc, hcp and – along the five-fold symmetry axes –

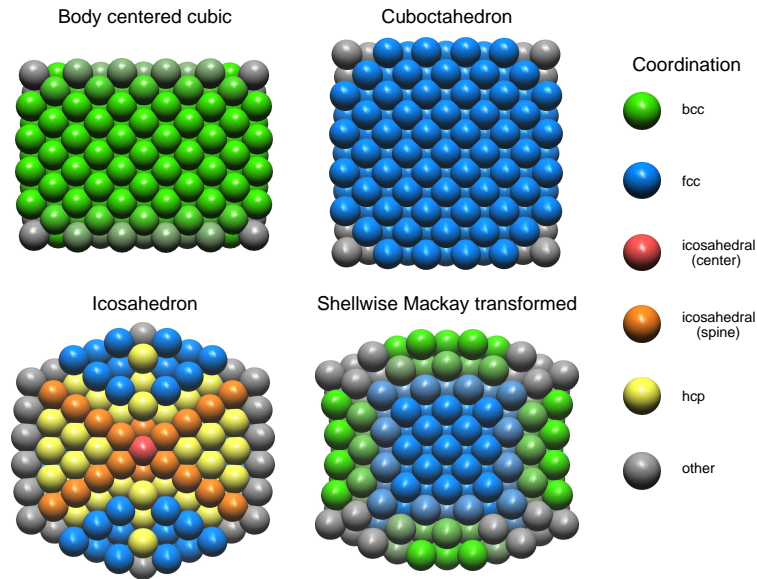


Figure 4. Cross sections of optimized geometries of 561 atom iron nanoparticles. The colour coding describes the local coordination of the atoms obtained by a common neighbour analysis. Bright colours refer to perfect matching of the CNA-signatures with the ideal bulk and surface configurations. With increasing number of deviations the colours turn into grey.

icosahedral environments. The SMT isomer, however, shows a rather unexpected pattern: While the central atoms are fcc coordinated according to the nearly completed Mackay-transformation of these shells, we find no trace of the typical icosahedral signatures in the outermost shells which, however, retain their overall icosahedral shape. Instead, their signatures show typical signs of an energetically favorable bcc-like coordination, accompanied by a pair distribution function which is rather typical for amorphous materials.<sup>12</sup>

#### 4 Morphologies of Fe-Pt and Co-Pt Nanoparticles

In the field of ultra-high density magnetic recording, the long-lasting exponential increase in storage density over time still seems unbroken. While eight years ago, densities of 35 GBit/in<sup>2</sup> were state of the art, recent lab demos reached values around 400 GBit/in<sup>2</sup> and the expectations of the manufacturers go up to 10 to 50 TBit/in<sup>2</sup> in the future. The main obstacle to further miniaturization is the so-called superparamagnetic limit, which threatens the long-time stability of the information stored.<sup>20</sup> The Néel relaxation time of a recording media grain is described by an exponential dependence on the product of anisotropy constant and volume divided by temperature. This imposes a lower boundary for the possible size above which the magnetization of a grain is (for a sufficiently long time) not affected by thermal relaxation processes. One widely discussed strategy to overcome this problem is the use of regular patterned arrays of nanoparticles, where one bit is essentially represented by one particle.<sup>3,4</sup> To obtain sufficiently small particles with thermally stable

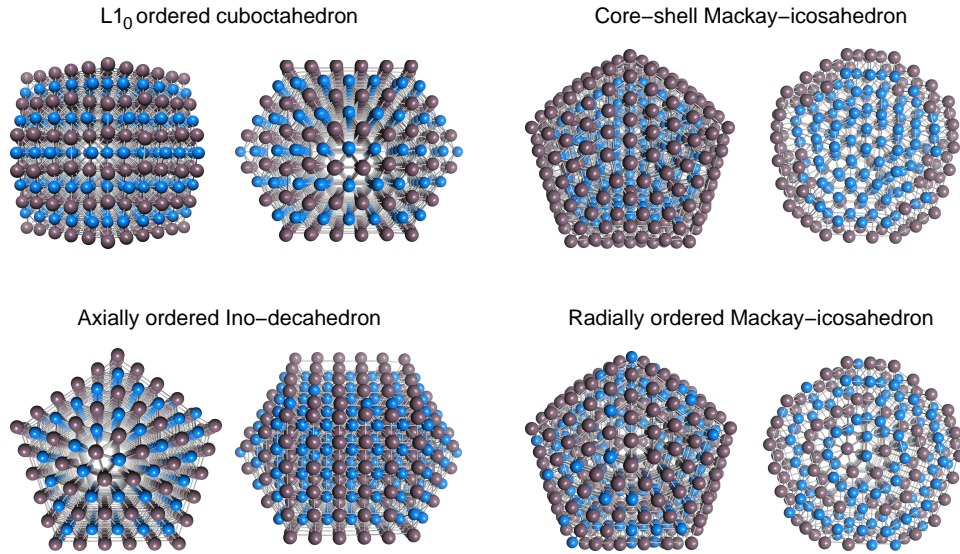


Figure 5. Various ordered morphologies of  $\text{Fe}_{265}\text{Pt}_{296}$  (or  $\text{Co}_{265}\text{Pt}_{296}$ , respectively) nanoparticles after structural relaxation in two different aspects. The blue spheres denote Fe (or Co) atoms, the brownish spheres Pt. The icosahedra are shown in cross section to visualize their inner structure.

magnetizations, near-stoichiometric FePt and CoPt alloys in the slightly tetragonally distorted  $L1_0$  phase are currently considered as the most promising materials, since their bulk anisotropy constants are about one order of magnitude larger than that of currently used media.<sup>20</sup> Considering these values, particle sizes of 4 nm or even smaller appear feasible.

The current production route is to fabricate disordered fcc FePt particles from gas phase experiments or wet-chemical production routes and obtain the ordered  $L1_0$  phase in a further annealing step.<sup>4</sup> However, it was reported recently that  $L1_0$  particles in the interesting size range with a sufficient magnetocrystalline anisotropy may be difficult to obtain in this way.<sup>21–23</sup> High resolution transmission electron microscopy (HRTEM) showed the occurrence of multiply twinned morphologies such as icosahedra and decahedra at diameters around 6 nm and below (e. g., 24, 25). These consist of several strained twins (20 in the case of Mackay-icosahedra and 5 for Ino-decahedra). Therefore such morphologies cannot be expected to exhibit a large uniaxial magnetocrystalline anisotropy even if the individual twins are perfectly  $L1_0$ -ordered, since they have different crystallographic orientations.

In order to shed more light on the origin of these problems, we started *ab initio* calculations of FePt and CoPt nanoparticles with of up 561 atoms ( $\approx 2.5$  nm in diameter), comparing nearly 60 configurations of particles of both materials with different sizes.<sup>26</sup> Although the largest particles are still too small to avoid superparamagnetism, general trends can be formulated from the results, as the largest clusters already possess a balanced surface-to-volume ratio (45 % at 2.5 nm as compared to 32 % at 4 nm). We find that disordered phases are considerably higher in energy than the desired  $L1_0$  phase. However, ordered multiply twinned morphologies are substantially more favorable throughout the investigated size range. The calculated energy differences can be as large as  $\Delta E = E - E_{L1_0} = -30$  meV/atom in the case of the radially ordered  $\text{Fe}_{265}\text{Pt}_{296}$  icosahedra.

dron, which is still close to thermal energies, but sizeable  $-90$  meV/atom for  $\text{Co}_{265}\text{Pt}_{296}$ . These results explain at least in part the experimental difficulties to obtain particles with large magnetocrystalline anisotropy at small sizes. The fully segregated icosahedron is a special case: It is with  $\Delta E = +20$  meV/atom higher in energy than the  $\text{L1}_0$  cuboctahedron in the case of  $\text{Fe}_{265}\text{Pt}_{296}$  but with  $\Delta E = -92$  meV/atom much more favorable in Co-Pt, pointing out strong segregation tendencies in the latter case.

## 5 Outlook

In this contribution, we wanted to demonstrate that large scale DFT calculations are a powerful tool providing information on material related properties on an atomistic level, which may not be obtained from experiment so far and can thus contribute significantly to the solution of unresolved questions in materials science and technology. Our ongoing work in the field of nanoparticles for ultra-high density recording applications includes the investigation of the size-dependence of the magnetocrystalline anisotropy energy of FePt and CoPt nanoparticles and the exploration of possible strategies to stabilize the  $\text{L1}_0$  phase by co-alloying with a third element. Considering the possibilities provided by the new Blue Gene/P at Jülich Supercomputing Centre (JSC), *ab initio* investigations of nanoparticles of 3.5 or even 4 nm, containing 1415 and 2057 atoms according to Eq. (1) and being of relevant size for technological applications, appear feasible in near future.

## Acknowledgments

We thank the John von Neumann Institute for Computing for granting computation time and support and, especially, P. Vezolle of IBM and I. Gutheil of JSC for their substantial efforts, making the VASP code run efficiently on the Blue Gene/L system. Financial support was granted by the Deutsche Forschungsgemeinschaft through SPP 1239 and SFB 445.

## References

1. I. M. L. Billas, A. Châtelain, and W. A. de Heer, *Magnetism from the atom to the bulk in iron, cobalt, and nickel clusters*, Science, **265**, 1682, 1994.
2. M. L. Tiago, Y. Zhou, M. M. G. Alemany, Y. Saad, and J. R. Chelikowsky, *Evolution of magnetism in iron from the atom to the bulk*, Phys. Rev. Lett., **97**, 147201, 2006.
3. S. Sun, C. B. Murray, D. Weller, L. Folks, and A. Moser, *Monodisperse FePt nanoparticles and ferromagnetic FePt nanocrystal superlattices*, Science, **287**, 1989, 2000.
4. S. Sun, *Recent advances in chemical synthesis, self-assembly, and applications of FePt nanoparticles*, Adv. Mater., **18**, 393, 2006.
5. P. Hohenberg and W. Kohn, *Inhomogeneous electron gas*, Phys. Rev., **136**, B864, 1964.
6. W. Kohn, “Electronic structure of matter – wave functions and density functionals”, in: Nobel Lectures, Chemistry 1996-2000, I. Grenthe, (Ed.), p. 213. World Scientific, Singapore, 2003.
7. G. Kresse and J. Furthmüller, *Efficient iterative schemes for ab initio total-energy calculations using a plane-wave basis set*, Phys. Rev. B, **54**, 11169, 1996.



8. G. Kresse and D. Joubert, *From ultrasoft pseudopotentials to the projector augmented-wave method*, Phys. Rev. B, **59**, 1758, 1999.
9. M. E. Gruner, G. Rollmann, S. Sahoo, and P. Entel, *Magnetism of close packed Fe<sub>147</sub> clusters*, Phase Transitions, **79**, 701, 2006.
10. M. E. Gruner, G. Rollmann, A. Hucht, and P. Entel, *Massively parallel density functional theory calculations of large transition metal clusters*, Lecture Series on Computer and Computational Sciences, **7**, 173, 2006.
11. G. Rollmann, M. E. Gruner, A. Hucht, P. Entel, M. L. Tiago, and J. R. Chelikowsky, *Shell-wise Mackay transformation in iron nano-clusters*, Phys. Rev. Lett., **99**, 083402, 2007.
12. M. E. Gruner, G. Rollmann, A. Hucht, and P. Entel, *Structural and magnetic properties of transition metal nanoparticles from first principles*, vol. 47 of *Advances in Solid State Physics*, Springer, Berlin, in press.
13. M. Pellarin, B. Baguenard, J. L. Vialle, J. Lerme, M. Broyer, J. Miller, and A. Perez, *Evidence for icosahedral atomic shell structure in nickel and cobalt clusters - comparison with iron clusters*, Chem. Phys. Lett., **217**, 349, 1994.
14. A. L. Mackay, *A dense non-crystallographic packing of equal spheres*, Acta Cryst., **15**, 916, 1962.
15. S. Ino, *Stability of multiply-twinned particles*, J. Phys. Soc. Jpn., **27**, 941, 1969.
16. D. L. Huber, *Synthesis, properties, and applications of iron nanoparticles*, Small, **1**, 482, 2005.
17. T. Vystavel, G. Palasantzas, S. A. Koch, and J. Th. M. De Hosson, *Nanosized iron clusters investigated with in situ transmission electron microscopy*, Appl. Phys. Lett., **82**, 197, 2003.
18. P. Bobadova-Parvanova, K. A. Jackson, S. Srinivas, and M. Horoi, *Density-functional investigations of the spin ordering in Fe<sub>13</sub> clusters*, Phys. Rev. B, **66**, 195402, 2002.
19. H. Jónsson and H. C. Andersen, *Icosahedral ordering in the Lennard-Jones liquid and glass*, Phys. Rev. Lett., **60**, 2295, 1988.
20. D. Weller and A. Moser, *Thermal effect limits in ultrahigh-density magnetic recording*, IEEE Trans. Magn., **35**, 4423, 1999.
21. B. Stahl, J. Ellrich, R. Theissmann, M. Ghafari, S. Bhattacharya, H. Hahn, N. S. Gajbhiye, D. Kramer, R. N. Viswanath, J. Weissmüller, and H. Gleiter, *Electronic properties of 4-nm FePt particles*, Phys. Rev. B, **67**, 014422, 2003.
22. T. Miyazaki, O. Kitakami, S. Okamoto, Y. Shimada, Z. Akase, Y. Murakami, D. Shindo, Y. K. Takahashi, and K. Hono, *Size effect on the ordering of L<sub>10</sub> FePt nanoparticles*, Phys. Rev. B, **72**, 144419, 2005.
23. O. Dmitrieva, B. Rellinghaus, J. Kästner, M. O. Liedke, and J. Fassbender, *Ion beam induced destabilisation of icosahedral structures in gas phase prepared FePt nanoparticles*, J. Appl. Phys., **97**, 10N112, 2005.
24. Z. R. Dai, S. Sun, and Z. L. Wang, *Shapes, multiple twins and surface structures of monodisperse FePt magnetic nanocrystals*, Surf. Sci., **505**, 325, 2002.
25. D. Sudfeld, O. Dmitrieva, N. Friedenberger, G. Dumpich, M. Farle, C. Song, C. Kisielowski, M. E. Gruner, and P. Entel, *HR-TEM studies of FePt nanoparticles by exit wave reconstruction*, Mater. Res. Soc. Symp. Proc., **998E**, 0998–J01–06, 2007.
26. M. E. Gruner, G. Rollmann, P. Entel, and M. Farle, *Multiply twinned morphologies of Fe-Pt and Co-Pt nanoparticles*, submitted.